

# The ground-state phase diagram for an alternative anisotropic extension of quantum spin-1 ferromagnetic biquadratic model

Yan-Wei Dai,<sup>1</sup> Qian-Qian Shi,<sup>1</sup> Xi-Hao Chen,<sup>2,1</sup> and Huan-Qiang Zhou<sup>1</sup>

<sup>1</sup>Centre for Modern Physics, Chongqing University, Chongqing 400044, The People's Republic of China

<sup>2</sup>Research Institute for New Materials and Technology,

Chongqing University of Arts and Sciences, Chongqing 400000, The People's Republic of China

The ground-state phase diagram is mapped out for an alternative anisotropic extension of quantum spin-1 ferromagnetic biquadratic model, which accommodates twelve distinct phases: three degenerate fractal phases, six Luttinger liquid phases and three symmetry-protected trivial phases. It is found that distinct types of quantum phase transitions are involved between them. In particular, one type arises from an instability of a Luttinger liquid towards a degenerate fractal phase, and the other type describes spontaneous symmetry breaking with type-B Goldstone modes from one degenerate fractal phase to another degenerate fractal phase, with the fractal dimension  $d_f$  being identical to the number of the type-B Goldstone modes, both of which turn out to be one. In addition, quantum phase transitions from the Luttinger liquid phases to the symmetry-protected trivial phases are identified to be in the Kosterlitz-Thouless universality class, with central charge being one.

PACS numbers:

## I. INTRODUCTION

Quantum critical phenomena continue to be a research subject of wide interest in condensed matter physics. In the Landau-Ginzburg-Wilson (LGW) paradigm, it is a basic notion of spontaneous symmetry breaking (SSB) [1] that makes it possible to classify distinct types of quantum phase transitions (QPTs) and quantum states of matter. However, many examples, which do not fall into this paradigm, are known even in one-dimensional quantum many-body systems, with the celebrated Haldane phase being a prominent example [2]. In fact, the Haldane phase is a typical example for the so-called symmetry-protected topological (SPT) phases [3, 4]. Further development unveils that there exist a class of the symmetry-protected trivial (SPt) phases [5], featuring that they are adiabatically connected to (unentangled) factorized states.

In addition, the Mermin-Wagner-Coleman theorem forbids continuous symmetries to be spontaneously broken for quantum many-body systems in one spatial dimension [6]. However, this is *only* valid for SSB with type-A Goldstone modes (GMs) [7, 8]. Instead, gapless low-lying excitations still survive strong quantum fluctuations, with their number being counted by central charge in conformal field theory [9]. More precisely, though (gapless) type-A GMs do not survive, their variants occur in the guise of gapless low-lying excitations in one-dimensional quantum many-body systems at criticality.

This scenario is observed in numerical simulations of one-dimensional quantum many-body systems in the context of the infinite Matrix Product State (iMPS) representation [10]. In practice, the algorithms, which yield a ground-state wave function in the iMPS representation, lead to infinitely degenerate ground states in a critical regime, due to the finiteness of the bond dimension, it thus results in pseudo SSB that vanishes as the bond dimension tends to infinity [10, 11]. This offers a powerful means to characterize the Kosterlitz-Thouless (KT) phase transitions [12], which describes the instability of a Luttinger liquid (LL) under a marginal perturbation, in the

context of tensor network simulations [13, 14].

In contrast, SSB with type-B GMs does occur in one spatial dimension [7]. As demonstrated in Refs. [15–17], this leads to scale-invariant quantum states of matter, so an abstract fractal underlies the ground-state subspace, characterized in terms of the fractal dimension introduced by Castro-Alvaredo and Doyon [18] (also cf. [19]) for the SU(2) Heisenberg ferromagnetic states. In fact, the fractal dimension may be identified with the number of type-B GMs. As a consequence, highly degenerate ground states arising from SSB with type-B GMs are scale-invariant, but not conformally invariant [15, 16], thus unveiling a deep connection between scale-invariant states and the counting rule of the GMs [7, 8].

Therefore, it is highly desirable to search for one-dimensional quantum many-body systems that exhibit distinct types of QPTs involving scale-invariant quantum states of matter. In this work, we investigate an alternative anisotropic extension of quantum spin-1 ferromagnetic biquadratic model, both numerically and analytically. It is different from an anisotropic extension of quantum spin-1 ferromagnetic biquadratic model studied in Ref. [15]. Numerical simulations are carried out in terms of infinite Time Evolving Block Decimation (iTEBD) [13]. The model exhibits twelve distinct phases, accommodating three degenerate fractal (DF) phases, six LL phases and three SPt phases. Two novel types of QPTs are unveiled: one type arises from the instabilities of the LL phases towards the DF phases, and the other type describes SSB with type-B GMs from one DF phase to another DF phase, with the fractal dimension  $d_f$  being identical to the number of type-B GMs  $N_B$ :  $d_f = N_B = 1$ . In addition, QPTs from the LL phases to the SPt phases are identified to be in the KT universality class, with central charge  $c$  being one.

## II. THE MODEL AND ITS DISTINCT PHASES

The Hamiltonian for an alternative anisotropic extension of quantum spin-1 ferromagnetic biquadratic model takes the

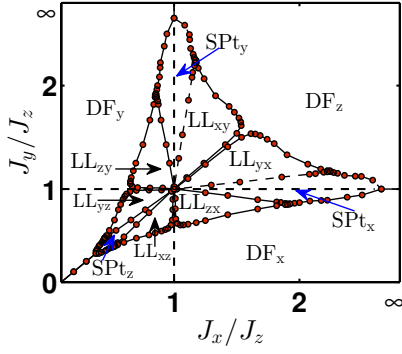


FIG. 1: (color online) The ground-state phase diagram for an alternative anisotropic extension of quantum spin-1 ferromagnetic biquadratic model (1), which accommodates the DF phases, the LL phases and the SPT phases in the region  $0 \leq J_x/J_z, 0 \leq J_y/J_z$ . Here, the bond dimension  $\chi$  is chosen to be  $\chi = 200$ .

form

$$H = \sum_j (J_x S_{x,j} S_{x,j+1} + J_y S_{y,j} S_{y,j+1} + J_z S_{z,j} S_{z,j+1})^4, \quad (1)$$

where  $S_{\mu,j}$  ( $\mu = x, y, z$ ) are the spin-1 operators at a lattice site  $j$ , and  $J_\mu$  denote the coupling parameters describing anisotropic interactions. Here, we remark that the sum over  $j$  is from 1 to  $L-1$  under the open boundary conditions (OBCs) and from 1 to  $L$  under the periodic boundary conditions (PBCs), with  $L$  being the system size. The model (1) features one symmetric transformation and two duality transformations, as a result of its invariance under a permutation with respect to  $x$ ,  $y$  and  $z$  (for more details, cf. Sec. A of the Supplementary Material (SM)). That is, the symmetric and duality transformations are induced from the symmetric group  $S_3$ , consisting of the permutations with respect to  $x$ ,  $y$  and  $z$ . As a consequence, one may set  $J_z$  as an energy scale and choose  $J_x$  and  $J_y$  as two independent coupling parameters.

The peculiarity of the model (1) is that the symmetry group varies with  $J_x$  and  $J_y$ . On the characteristic line  $J_x = J_y$ , the model (1) possesses the staggered  $SU(2)$  symmetry group and the staggered  $U(1)$  symmetry group, generated by  $K_x$ ,  $K_y$  and  $K_z$ , and  $R_x$ ,  $R_y$ , and  $R_z$ , respectively:  $K_x = \sum_j K_{x,j}$ ,  $K_y = \sum_j K_{y,j}$  and  $K_z = \sum_j K_{z,j}$ , with  $K_{x,j} = \sum_j (-1)^j [S_{x,j}^2 - S_{y,j}^2]/2$ ,  $K_{y,j} = \sum_j (-1)^j (S_{x,j} S_{y,j} + S_{y,j} S_{x,j})/2$  and  $K_{z,j} = \sum_j S_{z,j}/2$ , and  $R_x = \sum_j (-1)^j (S_{z,j})^2$ . Here, the generators  $K_x$ ,  $K_y$  and  $K_z$  satisfy the commutation relations:  $[K_\alpha, K_\beta] = i \varepsilon_{\alpha\beta\gamma} K_\gamma$ , where  $\varepsilon_{\alpha\beta\gamma}$  is a completely antisymmetric tensor, with  $\varepsilon_{xyz} = 1$ , and  $\alpha, \beta, \gamma = x, y, z$ . Meanwhile, a staggered  $SU(2)$  symmetry group and a staggered  $U(1)$  symmetry group also occur on the characteristic lines  $J_y = J_z$  and  $J_x = J_z$ , due to the symmetric and duality transformations induced from the symmetric group  $S_3$ . In particular, the staggered  $SU(3)$  symmetry group emerges at the isotropic point  $J_x = J_y = J_z$ . Given the staggered nature of the symmetry groups, we restrict ourselves to even  $L$ 's. More details about the symmetry groups are described in Sec. B of the SM.

Therefore, we may restrict ourselves to the region  $J_x/J_z \geq 0$ ,  $J_y/J_z \geq 0$  and  $J_z = 1$ . In fact, the region is partitioned

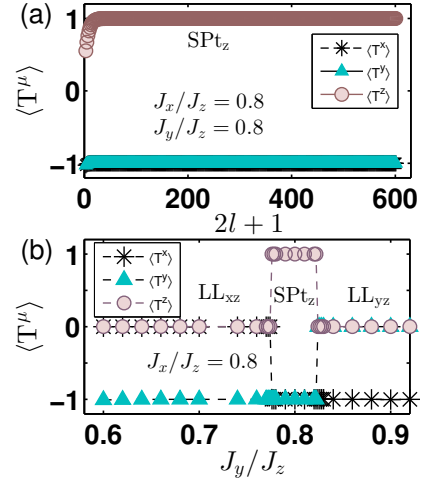


FIG. 2: (color online) (a) The non-local order parameter  $\langle T^\mu \rangle$  as a function of the block size  $2l+1$  from the iTEBD simulations, with the bond dimension  $\chi = 60$ , for an alternative anisotropic extension of quantum spin-1 ferromagnetic biquadratic model (1), with  $J_x/J_z = 0.8$  and  $J_y/J_z = 0.8$ , in the  $SPT_z$  phase. (b) The non-local order parameter  $\langle T^\mu \rangle$  as a function of  $J_y/J_z$  for fixed  $J_x/J_z = 0.8$  from the iTEBD simulations, with the bond dimension  $\chi = 60$ , which may be used to detect QPT points.

into six different regimes, which are symmetric or dual to each other, as a result of the symmetric and duality transformations. Hence, we only need to focus on one of the six regimes to perform numerical simulations of the model and map out the ground-state phase diagram. This regime is chosen to be  $0 \leq J_x \leq J_z$  and  $0 \leq J_y \leq J_z$ . The numerical simulations have been carried out in terms of the iTEBD [13], with the bond dimension  $\chi$  being  $\chi = 200$ . We plot the ground-state phase diagram in Fig. 1, which accommodates the twelve distinct phases: three DF phases, labeled as  $DF_x$ ,  $DF_y$  and  $DF_z$ , six LL phases, labeled as  $LL_{xy}$ ,  $LL_{yz}$ ,  $LL_{zx}$ ,  $LL_{yx}$ ,  $LL_{xz}$  and  $LL_{zy}$ , and three SPT phases, labeled as  $SPT_x$ ,  $SPT_y$  and  $SPT_z$ , respectively. We remark that the phase boundaries are determined from the entanglement entropy [20] and the ground-state fidelity per lattice site [21]. In addition, QPTs between the LL phases and the SPT phases are identified to be in the KT universality class with central charge  $c = 1$ , which arise from the instabilities of the LL phases towards the SPT phases.

### III. CHARACTERIZATION OF THE DISTINCT PHASES

Now we turn to the characterization of the SPT phases, the LL phases and the DF phases.

#### A. The SPT phases

A local order parameter, with a non-zero value, depicts a quantum state of matter with symmetry-breaking order. However, not all of quantum states of matter are subject to this description. A remarkable example is the SPT phases [5], which

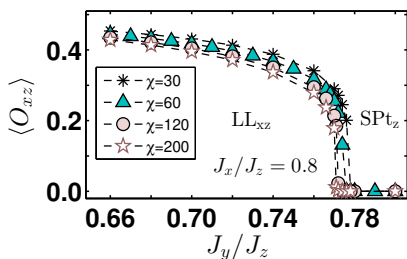


FIG. 3: (color online) The pseudo order parameter  $\langle O_{xz} \rangle$  as a function of  $J_y/J_z$  for fixed  $J_x/J_z = 0.8$ , with the bond dimension  $\chi = 30, 60, 120$  and  $200$ , respectively. The pseudo phase transition points between the LL<sub>xz</sub> phase and the SPt<sub>z</sub> phase are located from the pseudo order parameter  $\langle O_{xz} \rangle$ .

requires to introduce a non-local order parameter, which is defined as the combined operation of the site-centered inversion symmetry with the  $\pi$ -rotation  $R^\mu = \exp(i\pi S^\mu)$  around the  $\mu$  axis ( $\mu = x, y, z$ ) in the spin space [5, 22]

$$T^\mu = \langle \psi | I_{(1,D)} R_{(1,D)}^\mu | \psi \rangle / \text{tr}(\lambda_A^2 \lambda_B^2), \quad (2)$$

where  $I$  is the site-centered inversion symmetry, namely  $j \rightarrow -j$ , and  $\lambda_A$  and  $\lambda_B$  denote the Schmidt decomposition coefficients for a ground-state wave function  $|\psi\rangle$ , with the block size being  $2l + 1$ . If the combined symmetry is retained,  $\langle T^\mu \rangle$  must be equal to  $\pm 1$ . In particular,  $\langle T^\mu \rangle = -1$  indicates that a non-trivial SPt phase is involved.

In Fig. 2(a), we plot the non-local order parameter  $\langle T^\mu \rangle$  as a function of the block size  $2l + 1$ , as a result of the iTEBD simulation, with the bond dimension  $\chi = 60$ , for the model (1) with  $J_x/J_z = 0.8$  and  $J_y/J_z = 0.8$ , located in the SPt<sub>z</sub> phase. Our numerical results show that the block size  $2l + 1$  should be large enough, to ensure that the non-local order parameter  $\langle T^\mu \rangle$  is saturated.

In Fig. 2(b), we plot the non-local order parameter  $\langle T^\mu \rangle$  as a function of  $J_y/J_z$  for fixed  $J_x/J_z = 0.8$ . In the SPt phase, the non-local order parameters take the value:  $T^x = -1$ ,  $T^y = -1$ , and  $T^z = 1$ . In the LL phase, pseudo SSB occurs. Hence, the non-local order parameters take the values:  $T^x = 0$ ,  $T^y = -1$ , and  $T^z = 0$  in the LL<sub>xz</sub> phase and  $T^x = -1$ ,  $T^y = 0$ , and  $T^z = 0$  in the LL<sub>yz</sub> phase, respectively. The results show that the non-local order parameters  $\langle T^\mu \rangle$  detect the (pseudo) phase transition points: one is located at  $J_y/J_z = 0.774$  on the boundary between the LL<sub>xz</sub> phase and the SPt<sub>z</sub> phase, and the other is located at  $J_y/J_z = 0.882$  on the boundary between the SPt<sub>z</sub> phase and the LL<sub>yz</sub> phase, respectively.

## B. The LL phases

According to the Mermin-Wagner-Coleman theorem, continuous symmetries are not spontaneously broken for quantum many-body systems in one spatial dimension [6]. However, this is *only* valid for SSB with type-A GMs (GMs) [7, 15]. Instead, gapless low-lying excitations still survive strong quantum fluctuations, with their number being counted by central charge  $c$ . More precisely, type-A GMs survive in the guise

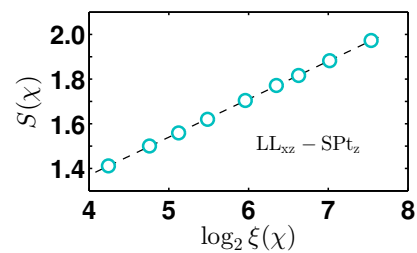


FIG. 4: (color online) The entanglement entropy  $S(\chi)$  versus  $\log_2 \xi(\chi)$  for fixed  $J_x/J_z = 0.7$ , at a transition point from the LL<sub>xz</sub> phase to the SPt<sub>z</sub> phase, as a result of the iTEBD simulations. Here, the bond dimension  $\chi$  ranges from 30 to 200.

of gapless low-lying excitations in conformal field theories. This scenario is observed [10, 11] in numerical simulations of one-dimensional quantum many-body systems in the context of the iTEBD algorithm [13]. In practice, such an algorithm leads to infinitely degenerate ground states in a critical regime, as a result of the finiteness of the bond dimension  $\chi$ . Hence, it results in pseudo SSB [10]. In order to keep consistency with the Mermin-Wagner-Coleman theorem, we introduce a pseudo-order parameter, which must be scaled down to zero, when the bond dimension  $\chi$  tends to infinity.

The Hamiltonian (1) possesses three U(1) symmetry groups in the entire parameter space, with only two of them being independent. In the LL phase, it is found that, pseudo SSB occurs for one of the three U(1), as a result of the finiteness of the bond dimension  $\chi$  in the iMPS representation. In the LL<sub>xz</sub> phase, this means that a pseudo local order parameter  $\langle O_{xz} \rangle = \langle S_j^x S_j^z \rangle$  emerges. In Fig. 3, we plot the pseudo order parameter  $\langle O_{xz} \rangle$  as a function of  $J_y/J_z$  for fixed  $J_x/J_z = 0.8$ , thus yielding a pseudo phase transition point from the LL<sub>xz</sub> phase to the SPt<sub>z</sub> phase, located at  $J_y/J_z = 0.776, 0.774, 0.771$  and  $0.77$ , with the bond dimension  $\chi = 30, 60, 120$  and  $200$ , respectively. When the bond dimension  $\chi$  tends to  $\infty$ , the pseudo order parameter  $\langle O_{xz} \rangle$  vanishes, as it should be.

In order to characterize a LL phase, we need to extract central charge  $c$ . One way to do so is to perform a finite-entanglement scaling analysis [23]

$$S(\chi) = \frac{c}{6} \log_2 \xi(\chi) + S_0(\chi), \quad (3)$$

where  $S_0(\chi)$  is an additive non-universal constant, and  $\xi(\chi) \sim \chi^\kappa$ , with  $\kappa$  being a finite-entanglement scaling exponent. The best linear fit is performed for four different points in the LL phase:  $(J_x/J_z, J_y/J_z) = (0.6, 0.5), (0.6, 0.8), (0.7, 0.8)$  and  $(0.8, 0.9)$ , respectively, with the bond dimension  $\chi$  ranging from 20 to 200. As a consequence, central charge  $c$  is estimated to be  $c = 1$ , with a relative error being less than 2%. Meanwhile, central charge  $c$  is extracted from a finite-size scaling analysis by exploiting a finite-size MPS algorithm under the periodic boundary conditions [24] (for more details, cf. Sec. C of the SM).

In addition, we focus on a QPT from the LL<sub>xz</sub> phase to the SPt<sub>z</sub> phase. The finite-entanglement scaling is performed for a pseudo critical point  $J_y/J_z$  to extract central charge  $c$ . In Fig. 4, we plot the entanglement entropy  $S(\chi)$  versus  $\log_2 \xi(\chi)$

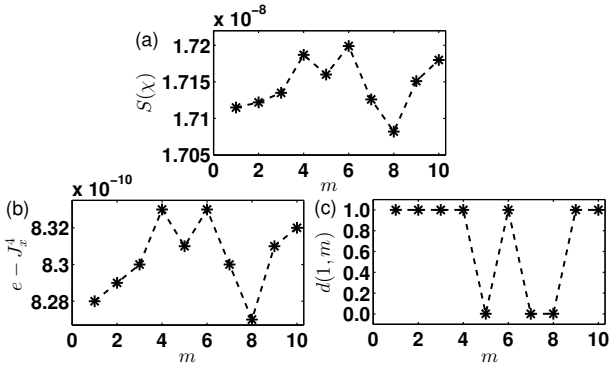


FIG. 5: (color online) (a) The entanglement entropy  $S(\chi)$ ; (b) The ground-state energy per lattice site  $e$ , with a constant  $J_x^4$  being subtracted; and (c) the ground-state fidelity  $d(1, m)$  per lattice site, with the ground state from the first random trial being a reference state. We present our results from the iTEBD simulations as a function of  $m$ , with  $m$  being the number of the random trials to choose different initial states. Here,  $J_x/J_z = 0.3$  and  $J_y/J_z = 0.8$  is chosen in the DF<sub>y</sub> phase, and the bond dimension  $\chi$  is  $\chi = 10$ .

for fixed  $J_x/J_z = 0.7$ , with the bond dimension  $\chi$  ranging from 30 to 200. The best linear fit is exploited to estimate central charge  $c = 1.0206$ , thus we conclude that the phase transition [12] from a critical phase to a gapful phase, which describes the instabilities of the LL under a marginal perturbation, is in the KT universality class, with central charge  $c = 1$ .

### C. The DF phases

In the DF<sub>y</sub> phase, we choose  $J_x/J_z = 0.3$  and  $J_y/J_z = 0.8$  to perform the iTEBD simulations. Here, the bond dimension  $\chi$  is chosen to be  $\chi = 10$ . Hence, one may generate a sequence of the ground states  $|\psi(k)\rangle$ , where  $k = 1, 2, \dots, m$ , with  $m$  being the number of the random trials to choose different initial states. In Fig. 5(a), we plot the entanglement entropy  $S(\chi)$  as a function of  $m$ . As we see, the entanglement entropy  $S(\chi)$  is negligible, with its numerical values being around  $10^{-8}$  in magnitude. That is, no entanglement is present in the DF<sub>y</sub> phase. In Fig. 5(b), we plot  $e - J_x^4$  as a function of  $m$ , with its values being around  $10^{-9}$  in magnitude. This implies that the ground-state energy per lattice site  $e$  is equal to  $J_x^4$  in the DF<sub>y</sub> phase. In addition, we choose the ground state  $|\psi(1)\rangle$  as a reference state, and define the ground-state fidelity per lattice site  $d(1, m)$  as follows [21]. The fidelity between  $|\psi(1)\rangle$  and  $|\psi(m)\rangle$  is  $F(|\psi(m)\rangle, |\psi(1)\rangle) = |\langle \psi(m) | \psi(1) \rangle|$ , which asymptotically scales as  $F(|\psi(m)\rangle, |\psi(1)\rangle) \sim d^L(1, m)$ , with  $L$  being the system size. In Fig. 5(c), we plot the ground-state fidelity per lattice site  $d(1, m)$  as a function of  $m$ , which appears to take two different values 1 and 0. This implies that there are two degenerate ground states in the DF<sub>y</sub> phase. Hence, our numerical results indicate that, in the DF phases, all the ground states are factorized states, with the ground-state degeneracy being two.

We turn to an analytical approach to the ground states in the DF<sub>y</sub> phase, away from the two characteristic lines  $J_y/J_z = 1$

with  $J_x/J_z > 0$  and  $J_x/J_z = 0$  with  $J_y/J_z > 0$ . The two degenerate ground states in the DF<sub>y</sub> phase, denoted as  $|\psi_g\rangle$ , take the form:  $|\psi_g\rangle = \bigotimes_l |0_y 0_z\rangle_l$  and  $|\psi_g\rangle = \bigotimes_l |0_z 0_y\rangle_l$  ( $l = 1, \dots, L/2$ ), where  $|0_y\rangle_{2l-1/2l}$  and  $|0_z\rangle_{2l-1/2l}$  are eigenvectors of the spin operators  $S_{y,2l-1/2l}$  and  $S_{z,2l-1/2l}$ , respectively, with an eigenvalue being zero. Note that the ground-state energy per lattice site  $e$  being equal to  $J_x^4$ , consistent with the numerical results from the iTEBD simulations. The ground-state degeneracy is two, due to the fact that the one-site translation symmetry is spontaneously broken in the DF<sub>y</sub> phase.

In particular, we are able to derive the ground-state wave functions on the characteristic line  $J_y/J_z = 1$  with  $J_x/J_z > 0$  (for more details, cf. Sec. D of the SM). Since the model possesses a staggered SU(2) symmetry group and a staggered U(1) symmetry group on the characteristic line  $J_y/J_z = 1$  with  $J_x/J_z > 0$ , SSB with type-B GMs arises, thus yielding highly degenerate ground states, with the number of type-B GMs  $N_B$  being one:  $N_B = 1$ . That is, an abstract fractal underlies the ground-state subspace, with the fractal dimension  $d_f$  being identical to the number of type-B GMs  $N_B$ . Combining with the symmetric and duality transformations induced from the symmetric group  $S_3$ , the staggered SU(3) symmetry group emerges at the isotropic point  $J_x = J_y = J_z$ . In fact, the model Hamiltonian (1) is unitarily equivalent to the staggered SU(3) ferromagnetic biquadratic model, as seen in Sec. B of the SM. Therefore, as shown in Ref. [17], the staggered SU(3) symmetry group is spontaneously broken to  $U(1) \times U(1)$ , thus yielding two type-B GMs, with the fractal dimension  $d_f$  being identical to the number of type-B GMs  $N_B$ :  $d_f = N_B = 2$ .

In addition, on the characteristic line  $J_x/J_z = 0$  with  $J_y/J_z > 0$ , a brute force calculation shows that a factorized ground state  $|\Psi_f\rangle$ , with the ground-state energy per lattice site  $e$  being equal to 0, takes the form

$$|v_1\rangle_{2l-1} = \sin \zeta |0_y\rangle_{2l-1} + e^{i\theta} \cos \zeta |1_y\rangle_{2l-1}, \quad (4)$$

$$|v_2\rangle_{2l} = \frac{J_y \cos \zeta}{\sqrt{J_y^2 \cos^2 \zeta + J_z^2 \sin^2 \zeta}} |0_y\rangle_{2l} + e^{-i\theta} \frac{J_z \sin \zeta}{\sqrt{J_y^2 \cos^2 \zeta + J_z^2 \sin^2 \zeta}} |1_y\rangle_{2l},$$

where  $\zeta$  and  $\theta$  are two free parameters that are real (for more details, cf. Sec. D of the SM). That is, the model (1) admits a two-parameter family of degenerate factorized ground states on the characteristic line  $J_x/J_z = 0$  with  $J_y/J_z > 0$ . Generically,  $|\Psi_f\rangle$  is not invariant under the one-site translation operation, indicating that the symmetry under the one-site translation operation is spontaneously broken.

Our discussions clearly show that the ground-state degeneracy is  $L+1$  on the characteristic lines  $J_x/J_z = 0$  and  $J_y/J_z = 1$ , and it is *only* two in the DF<sub>y</sub> phase away from the two characteristic lines, though they are in the *same* DF<sub>y</sub> phase. This observation challenges the conventional wisdom, which dictates that it is always possible to adiabatically connect ground-state wave functions at any two points, as long as they are in the *same* phase.

## IV. NOVEL TYPES OF QUANTUM PHASE TRANSITIONS

Two novel types of QPTs are unveiled. The first type arises from the instabilities of the LL phases towards the DF phases.

This type of QPTs is similar to the celebrated Pokrovsky-Talapov (PT) transitions [25], with a remarkable difference that the ground-state degeneracy is, generically, two in the DF phases. In contrast, the PT transitions describe the instabilities of the LL phases towards an unentangled state, with the ground-state degeneracy being one. In both cases, no entanglement is present in a ground-state wave function that may be attributed to a (trivial) scale-invariant state, with the fractal dimension  $d_f = 0$  [26].

The second type describes SSB with type-B GMs from one DF phase to another DF phase, with the fractal dimension  $d_f$  being identical to the number of type-B GMs  $N_B$ . We remark that the Hamiltonian (1) possesses the staggered SU(2) symmetry group, generated by  $K_x$ ,  $K_y$  and  $K_z$ , in addition to the U(1) symmetry group, generated by  $R_z$ , on the characteristic line  $J_x = J_y$ . We remark that the staggered SU(2) symmetry group is spontaneously broken to U(1), with the U(1) symmetry group, generated by  $R_z$ , being left intact. Accordingly, one may define the raising operator  $K_+ = \sum_j K_{+,j}$  and the lowering operator  $K_- = \sum_j K_{-,j}$ , with  $K_{\pm,j} = (K_{x,j} \pm iK_{y,j})/\sqrt{2}$ . They satisfy the commutation relations:  $[K_z, K_+] = K_+$ ,  $[K_+, K_-] = K_z$  and  $[K_-, K_z] = K_-$ .

We choose  $|hws\rangle = (|0_x 0_z \dots 0_x 0_z\rangle + |0_y 0_z \dots 0_y 0_z\rangle)/\sqrt{2}$  as the highest weight state, which is invariant under the two-site translation. Here,  $|0_x\rangle/|0_y\rangle$  is the eigenvector of  $S_{x,j}/S_{y,j}$ , with the eigenvalue being 0. The interpolating fields are  $K_{+,j}$  and  $K_{-,j}$ , for the generator  $K_-$  and the generator  $K_+$ , respectively. Thus,  $\langle K_{z,j} \rangle$  is the local order parameter, given that  $\langle [K_{+,j}, K_-] \rangle = \langle [K_+, K_{-,j}] \rangle = \langle K_{z,j} \rangle \neq 0$ . Therefore, the two generators  $K_-$  and  $K_+$  are broken. According to the counting rule [7], the number of type-B GMs  $N_B$  is one:  $N_B = 1$ .

As demonstrated in Ref. [16], for a given filling  $f = M/L$ , the entanglement entropy  $S_f(n)$  take the form

$$S_f(n) = \frac{N_B}{2} \log_2 n + S_{0f}, \quad (5)$$

where  $S_{0f}$  is an additive non-universal constant. An analytical treatment is presented for  $S_f(n)$  in Sec. E of the SM, confirming this scaling relation, with  $N_B = 1$ . Combining with a

field-theoretic prediction that the prefactor is half the fractal dimension  $d_f$  [18], we conclude that the fractal dimension  $d_f$  is identical to the number of type-B GMs  $N_B$ :  $d_f = N_B$ .

## V. SUMMARY

An extensive numerical simulation has been performed for an alternative anisotropic extension of quantum spin-1 ferromagnetic biquadratic model in terms of the iTEBD algorithm. The ground-state phase diagram accommodates the twelve distinct phases: three DF phases, six LL phases, and three SPT phases. In addition, an analytical approach to the DF phases has been developed to unveil a deep connection between scale-invariant states, which appear to be highly degenerate ground states arising from SSB with type-B GMs, and the counting rule of the GMs. Meanwhile, the phase boundaries have been determined from the entanglement entropy and the ground-state fidelity per lattice site.

As it turns out, QPTs between the LL phases and the SPT phases are identified to be in the KT universality class with central charge  $c = 1$ , which arise from the instabilities of the LL phases towards the SPT phases. In particular, two novel types of QPTs are unveiled: one type arises from an instability of a LL phase towards a DF phase, and the other type describes SSB with type-B GMs from one DF phase to another DF phase, with the fractal dimension  $d_f$  being identical to the number of type-B GMs  $N_B$ :  $d_f = N_B = 1$ , on the characteristic line  $J_x = J_y$  between the DF<sub>x</sub> phase and DF<sub>y</sub> phase, and  $d_f = N_B = 2$  at the characteristic (isotropic) point  $J_x = J_y = J_z$ . Our results challenge the conventional wisdom that it is always possible to adiabatically connect any two ground-state wave functions, as long as they are in the *same* phase. In fact, the ground-state degeneracies may be different for two points in the *same* phase, as it happens in the DF phases.

*Acknowledgements.* We thank Murray Batchelor, John Fjærrestad and Ian McCulloch for enlightening discussions.

- 
- [1] P. W. Anderson, Basic Notions Condensed Matter Physics, Addison-Wesley: The Advanced Book Program (Addison-Wesley, Reading, MA, 1997).
  - [2] F. D. M. Haldane, Phys. Lett. A **93**, 464 (1983); F. D. M. Haldane, Phys. Rev. Lett. **50**, 1153 (1983).
  - [3] X. Chen, Z.-C. Gu, and X.-G. Wen, Phys. Rev. B **83**, 0355107 (2011); X. Chen, Z.-C. Gu, and X.-G. Wen, Phys. Rev. B **84**, 235128 (2011).
  - [4] F. Pollmann and A. M. Turner, Phys. Rev. B **86**, 125441 (2012); F. Pollmann, E. Berg, A. M. Turner, and M. Oshikawa, Phys. Rev. B **85**, 075125 (2012); F. Pollmann and A. M. Turner, Phys. Rev. B **86**, 125441 (2012).
  - [5] Y. Fuji, F. Pollmann, and M. Oshikawa, Phys. Rev. Lett. **114**, 177204 (2015).
  - [6] N. D. Mermin and H. Wagner, Phys. Rev. Lett. **17**, 1133 (1966); S. R. Coleman, Commun. Math. Phys. **31**, 259 (1973).
  - [7] H. Watanabe and H. Murayama, Phys. Rev. Lett. **108**, 251602 (2012); H. Watanabe and H. Murayama, Phys. Rev. X **4**, 031057 (2014).
  - [8] Y. Nambu, J. Stat. Phys. **115**, 7 (2004).
  - [9] P. D. Francesco, P. Mathieu, and D. Sénéchal, Conformal Field Theory (Springer, Berlin, 1997).
  - [10] H.-L. Wang, J.-H. Zhao, B. Li, and H.-Q. Zhou, J. Stat. Mech. L10001 (2011); H.-L. Wang, A.-M. Chen, B. Li, and H.-Q. Zhou, J. Phys. A: Math. Theor. **45** 015306 (2012).
  - [11] Y.-W. Dai, B.-Q. Hu, J.-H. Zhao, and H.-Q. Zhou, J. Phys. A: Math. Theor. **43**, 372001 (2010); H.-L. Wang, Y.-W. Dai, B.-Q. Hu, and H.-Q. Zhou, Phys. Lett. A **375**, 4045 (2011).
  - [12] V. L. Berezinskii, Sov. Phys. JETP **34**, 610 (1991); J. M. Kosterlitz and D. J. Thouless, J. Phys. C **6**, 1181 (1973).
  - [13] G. Vidal, Phys. Rev. Lett. **98**, 070201 (2007).
  - [14] I. P. McCulloch, J. Stat. Mech. **2007**, P10014 (2007); F.

- Heidrich-Meisner, I. P. McCulloch, and A. K. Kolezhuk, *Phys. Rev. B* **81**, 179902 (2010).
- [15] Q.-Q. Shi, Y.-W. Dai, S.-H. Li, and H.-Q. Zhou, arXiv:2204.05692 (2022).
- [16] Q.-Q. Shi, Y.-W. Dai, H.-Q. Zhou, and I. P. McCulloch, arXiv: 2201.01071 (2022).
- [17] H.-Q. Zhou, Q.-Q. Shi, I. P. McCulloch, and M. T. Batchelor, arXiv: 2302.13126 (2023).
- [18] O. A. Castro-Alvaredo and B. Doyon, *J. Stat. Mech.*, 2011(02): P02001 (2011); O. A. Castro-Alvaredo and B. Doyon, *Phys. Rev. Lett.* **108**, 120401 (2012).
- [19] V. Popkov and M. Salerno, *Phys. Rev. A* **71**, 012301 (2005).
- [20] G. Vidal, J. I. Latorre, E. Rico, and A. Kitaev, *Phys. Rev. Lett.* **90**, 227902 (2003).
- [21] H.-Q. Zhou and J. P. Barjaktarevič, *J. Phys. A: Math. Theor.* **41** 412001 (2008); H.-Q. Zhou, R. Orús, and G. Vidal, *Phys. Rev. Lett.* **100**, 080601 (2008).
- [22] X.-H. Chen, I. P. McCulloch, M. T. Batchelor, and H.-Q. Zhou, *Phys. Rev. B.* **102**, 085146 (2020).
- [23] L. Tagliacozzo, T. R. de Oliveira, S. Iblisdir, and J. I. Latorre, *Phys. Rev. B* **78**, 024410 (2008); F. Pollmann, S. Mukerjee, A. M. Turner, and J. E. Moore, *Phys. Rev. Lett.* **102**, 255701 (2009).
- [24] F. Verstraete, D. Porras, and J. I. Cirac, *Phys. Rev. Lett.* **93**, 227205 (2004).
- [25] V. L. Pokrovsky and A. L. Talapov, *Phys. Rev. Lett.* **42**, 65 (1979).
- [26] H.-Q. Zhou, Q.-Q. Shi, and Y.-W. Dai, *Entropy*, **24**, 1306 (2022).

## Supplementary Material

### A. Symmetric and duality transformations

We restrict ourselves to the region  $J_x/J_z \geq 0$ ,  $J_y/J_z \geq 0$  and  $J_z = 1$ . This is due to the fact that the Hamiltonian (1) is invariant under permutations with respect to  $x$ ,  $y$  and  $z$ , which induces symmetric and duality transformations from the symmetric group  $S_3$ .

For simplicity, we define the variables  $X = J_x/J_z$  and  $Y = J_y/J_z$ . Hence, the Hamiltonian (1) is re-parametrized as  $H(X, Y)$ . The Hamiltonian  $H(X, Y)$  satisfies the following two dualities:

(i) The Hamiltonian  $H(X, Y)$  is dual to the Hamiltonian  $H(X', Y')$  under a local unitary transformation  $U_1$ :  $S_{x,j} \rightarrow -S_{x,j}$ ,  $S_{y,j} \rightarrow S_{z,j}$  and  $S_{z,j} \rightarrow S_{y,j}$ . Hence, we have  $H(X, Y) = k(X, Y)U_1H(X', Y')U_1^\dagger$ , with  $X' = X/Y$ ,  $Y' = 1/Y$  and  $k(X, Y) = 1/Y^2$ . The Hamiltonian is invariant on the characteristic line  $Y = 1$ .

(ii) The Hamiltonian  $H(X, Y)$  is dual to the Hamiltonian  $H(X', Y')$  under a local unitary transformation  $U_2$ :  $S_{x,j} \rightarrow S_{z,j}$ ,  $S_{y,j} \rightarrow -S_{y,j}$  and  $S_{z,j} \rightarrow S_{x,j}$ . Hence, we have  $H(X, Y) = k(X, Y)U_2H(X', Y')U_2^\dagger$ , with  $X' = 1/X$ ,  $Y' = Y/X$  and  $k(X, Y) = X^2$ . The Hamiltonian is invariant on the characteristic line  $X = 1$ .

In addition, the Hamiltonian  $H(X, Y)$  is symmetric with respect to  $X = Y$  under a local unitary transformation  $U_0$ :  $S_{x,j} \rightarrow S_{y,j}$ ,  $S_{y,j} \rightarrow S_{x,j}$  and  $S_{z,j} \rightarrow -S_{z,j}$ .

The presence of the symmetric and duality transformations separates the region ( $X \geq 0$  and  $Y \geq 0$ ) into six distinct regimes, as shown in Fig. S1, which are symmetric or dual to each other.

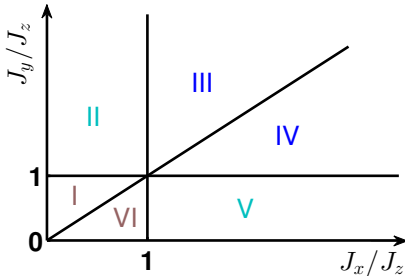


FIG. S1: (color online) The six regimes, symmetric or dual to each other, in the region  $J_x/J_z \geq 0$  and  $J_y/J_z \geq 0$  for an alternative anisotropic extension of quantum spin-1 ferromagnetic biquadratic model.

### B. The variation of the symmetry group with the coupling parameters

In the entire region  $J_x/J_z \geq 0$  and  $J_y/J_z \geq 0$ , the model Hamiltonian (1) possesses three  $U(1)$  symmetry groups, generated by  $G_x$ ,  $G_y$  and  $G_z$ , with  $G_x = \sum_j (-1)^j [(S_{x,j})^2 - (S_{y,j})^2]$ ,  $G_y = \sum_j (-1)^j [(S_{y,j})^2 - (S_{z,j})^2]$  and  $G_z = \sum_j (-1)^j [(S_{z,j})^2 -$

$(S_{j,x})^2]$ , respectively. However, only two of them are independent, due to the fact that  $G_x + G_y + G_z = 0$ . Hence, the symmetry group at a generic point is  $U(1) \times U(1)$ .

The Hamiltonian (1) possesses three characteristic lines, defined as  $J_x = J_y$ ,  $J_y = J_z$  and  $J_z = J_x$ , respectively. On each of the three characteristic lines, the symmetry group is enlarged to  $SU(2) \times U(1)$ . Given that the three characteristic lines are cyclic under the symmetric group  $S_3$ , consisting of the permutations with respect to  $x$ ,  $y$  and  $z$ , one only needs to focus on one of them. For an illustration, we choose the characteristic line  $J_x = J_y$ . The staggered  $SU(2)$  symmetry group is generated by  $K_x = \sum_j K_{x,j}$ ,  $K_y = \sum_j K_{y,j}$  and  $K_z = \sum_j K_{z,j}$ , with  $K_{x,j} = \sum_j (-1)^j [S_{x,j}^2 - S_{y,j}^2]/2$ ,  $K_{y,j} = \sum_j (-1)^j (S_{x,j}S_{y,j} + S_{y,j}S_{x,j})/2$  and  $K_{z,j} = \sum_j S_{z,j}/2$ , and the  $U(1)$  symmetry group is generated by  $R_z = \sum_j (-1)^j (S_{z,j})^2$ . We remark that, in three cases, the generators  $K_x$ ,  $K_y$  and  $K_z$  satisfy the commutation relations:  $[K_\alpha, K_\beta] = i\varepsilon_{\alpha\beta\gamma}K_\gamma$ , where  $\varepsilon_{\alpha\beta\gamma}$  ( $\alpha, \beta, \gamma = x, y, z$ ) is a completely antisymmetric tensor, with  $\varepsilon_{xyz} = 1$ .

In addition, the staggered  $SU(3)$  symmetry group [S1, S2] emerges at the characteristic (isotropic) point  $J_x = J_y = J_z$ , which is realized in terms of the spin-1 operators:  $J_\alpha = \sum_j J_\alpha^j$  ( $\alpha = 1, 2, \dots, 8$ ), with  $J_1 = 1/2 \sum_j S_{x,j}$ ,  $J_2 = 1/2 \sum_j S_{y,j}j^y$ ,  $J_3 = 1/2 \sum_j S_{z,j}$ ,  $J_4 = 1 - 3/2 \sum_j (-1)^j (S_{z,j})^2$ ,  $J_5 = 1/2 \sum_j (-1)^j [(S_{x,j})^2 - (S_{y,j})^2]$ ,  $J_6 = 1/2 \sum_j (-1)^j (S_{y,j}S_{z,j} + S_{z,j}S_{y,j})$ ,  $J_7 = 1/2 \sum_j (-1)^j (S_{z,j}S_{x,j} + S_{x,j}S_{z,j})$  and  $J_8 = 1/2 \sum_j (-1)^j (S_{x,j}S_{y,j} + S_{y,j}S_{x,j})$ .

It appears to be proper to point out a connection of the model Hamiltonian (1) with the well-studied spin-1 ferromagnetic bilinear-biquadratic model [S3]. In fact, the spin-1 bilinear-biquadratic model accommodates the staggered  $SU(3)$  ferromagnetic biquadratic model, which in turn is the isotropic limit of an alternative anisotropic extension of quantum spin-1 ferromagnetic biquadratic model, investigated in Ref. [S2]:

$$\mathcal{H} = \sum_j (\mathcal{J}_x S_{x,j} S_{x,j+1} + \mathcal{J}_y S_{y,j} S_{y,j+1} + \mathcal{J}_z S_{z,j} S_{z,j+1})^2. \quad (\text{S1})$$

At the isotropic point  $J_x = J_y = J_z = J$  or  $\mathcal{J}_x = \mathcal{J}_y = \mathcal{J}_z = \mathcal{J}$ , the model Hamiltonian (1)  $H$  and the Hamiltonian  $\mathcal{H}$  (S1) satisfy the relationship:  $H = J^4 (5\mathcal{H} | \mathcal{J}^2 - 4)$ , up to a unitary transformation. As it turns out, the model Hamiltonian (1) at the isotropic point  $J_x = J_y = J_z$  is unitarily equivalent to the staggered  $SU(3)$  ferromagnetic biquadratic model (S1). In this sense, one may regard the model Hamiltonian (1) as an alternative anisotropic extension of quantum spin-1 ferromagnetic biquadratic model. Actually, the Hamiltonian (S1) shares exactly the same symmetric and duality transformations induced from the symmetric group  $S_3$  as the Hamiltonian (1). Indeed, the model (S1) on the characteristic lines  $\mathcal{J}_x = \mathcal{J}_y$ ,  $\mathcal{J}_y = \mathcal{J}_z$  and  $\mathcal{J}_x = \mathcal{J}_z$  shares the same symmetry group as the model Hamiltonian (1) on the characteristic lines  $J_x = J_y$ ,  $J_y = J_z$  and  $J_x = J_z$ . Hence,

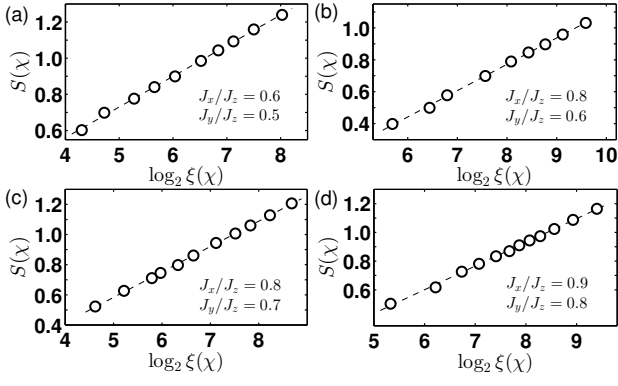


FIG. S2: (color online) The entanglement entropy  $S(\chi)$  versus correlation length  $\xi(\chi)$  for four different points  $(J_x/J_z, J_y/J_z) = (0.6, 0.5)$ ,  $(0.8, 0.6)$ ,  $(0.8, 0.7)$  and  $(0.9, 0.8)$  in the  $\text{LL}_{xz}$  phase, with the bond dimension ranging from 20 to 200.

TABLE S1: Central charge  $c$  is extracted to be  $c = 1$  in the LL phase from the iTEBD simulations. Here, we have chosen  $(J_x/J_z, J_y/J_z) = (0.6, 0.5)$ ,  $(0.8, 0.6)$ ,  $(0.8, 0.7)$  and  $(0.9, 0.8)$ , respectively.

|     | $J_x/J_z = 0.6$ | $J_x/J_z = 0.8$ | $J_x/J_z = 0.8$ | $J_x/J_z = 0.9$ |
|-----|-----------------|-----------------|-----------------|-----------------|
|     | $J_y/J_z = 0.5$ | $J_y/J_z = 0.6$ | $J_y/J_z = 0.7$ | $J_y/J_z = 0.8$ |
| $c$ | 1.017           | 0.9906          | 1.0122          | 0.9906          |

both of the models in the isotropic limit share the same staggered  $\text{SU}(3)$  symmetry group. As a consequence, one may conclude that the SSB pattern from  $\text{SU}(2)$  to  $\text{U}(1)$  occurs for the model Hamiltonian (1) on the characteristic line  $J_y = J_z$  ( $0 < J_x/J_z < 1$ ) and on the characteristic line  $J_x = J_y$  with  $0 < J_x/J_z < J_x^c$ , with the number of type-B GMs  $N_B$  being one, and that the SSB pattern from  $\text{SU}(3)$  to  $\text{U}(1) \times \text{U}(1)$  occurs for the model Hamiltonian (1) at the isotropic point  $J_x = J_y = J_z$ , with the number of type-B GMs  $N_B$  being two, respectively.

### C. Extracting central charge $c$ from the entanglement entropy in the LL phases

Here, central charge  $c$  is extracted from the iTEBD simulation [S4] and from the finite-size MPS simulations under the PBCs [S5] in the LL phases.

#### 1. Central charge $c$ from the iTEBD simulations in the LL phases

In the iMPS representation, the entanglement entropy  $S$  [S6], as a measure of bipartite entanglement, is written as  $S = -\sum_{i=1}^{\chi} \lambda_i^2 \log_2 \lambda_i^2$ , with  $\lambda_i$  being the singular values. Central charge  $c$  in a critical regime is estimated from a finite-entanglement scaling analysis (3).

For a given value of the bond dimension  $\chi$ , the correlation length  $\xi$  is defined in terms of the ratio between the largest and second largest eigenvalues of the transfer ma-

TABLE S2: Central charge  $c$  is extracted to be  $c = 1$  in the LL phase from the finite-size MPS simulations under the PBCs, with an error being less than 4%. Here, we have chosen  $(J_x/J_z, J_y/J_z) = (0.6, 0.5)$ ,  $(0.8, 0.6)$ ,  $(0.8, 0.7)$  and  $(0.9, 0.8)$ , with the system size  $L = 50$  and the bond dimension  $\chi = 30$ .

|     | $J_x/J_z = 0.6$ | $J_x/J_z = 0.8$ | $J_x/J_z = 0.8$ | $J_x/J_z = 0.9$ |
|-----|-----------------|-----------------|-----------------|-----------------|
|     | $J_y/J_z = 0.5$ | $J_y/J_z = 0.6$ | $J_y/J_z = 0.7$ | $J_y/J_z = 0.8$ |
| $c$ | 1.029           | 1.008           | 1.034           | 0.9693          |

trix:  $1/\xi(\chi) = \log_2 |\epsilon_0(\chi)/\epsilon_1(\chi)|$ . In order to characterize the LL phases, we choose four different points  $(J_x/J_z, J_y/J_z) = (0.6, 0.5)$ ,  $(0.8, 0.6)$ ,  $(0.8, 0.7)$  and  $(0.9, 0.8)$  in the  $\text{LL}_{xz}$  phase. The finite-entanglement scaling analysis is performed, with the bond dimension ranging from 20 to 200. In Fig. S2, the best linear fit is exploited to estimate central charge  $c$ , listed in Table S1. The iTEBD simulations yield that central charge is  $c = 1$  in the  $\text{LL}_{xz}$  phase, with a relative error being less than 2%.

#### 2. Central charge $c$ from the finite-size simulations in the LL phases

We are also able to extract central charge  $c$  from numerical simulations of the model (1) in the LL phases in terms of the finite-size MPS algorithm for quantum many-body systems under the PBCs [S5].

A quantum many-body system, with the system size being  $L$ , is partitioned into a block  $n$  and its environment  $L - n$ , respectively. Then, central charge  $c$  may be extracted from a scaling relation for the entanglement entropy  $S(n)$  under the PBCs [S7]:

$$S(n) = \frac{c}{3} T(n) + S_0, \quad (\text{S2})$$

where  $S_0$  is an additive non-universal constant, and  $T(n)$  is a universal scaling function, defined as

$$T(n) = \log_2 \left( \frac{L}{\pi} \sin \frac{\pi n}{L} \right). \quad (\text{S3})$$

We choose four different points  $(J_x/J_z, J_y/J_z) = (0.6, 0.5)$ ,  $(0.8, 0.6)$ ,  $(0.8, 0.7)$  and  $(0.9, 0.8)$  in the  $\text{LL}_{xz}$  phase, with the system size  $L = 50$ . The simulations are performed in terms of the finite-size MPS algorithm under the PBCs [S5], with the bond dimension  $\chi = 30$ . In Fig. S3, the best linear fit is performed to estimate central charge  $c$ , listed in Table S2, with a relative error being less than 4%. Therefore, the finite-size simulation results lend further support to our conclusion that the  $\text{LL}_{xz}$  phase is critical, with central charge being one.

### D. The factorized ground states in the DF phases: on and away from the characteristic lines

We emphasize that the Hamiltonian (1) is invariant under permutations with respect to  $x$ ,  $y$  and  $z$ , which induce symmetric and duality transformations from the symmetric group

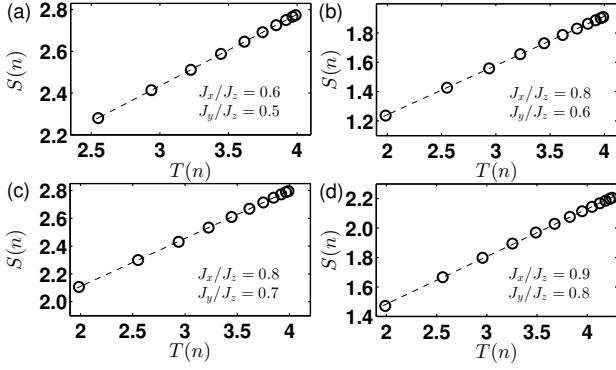


FIG. S3: (color online) A finite block-size scaling analysis of the entanglement entropy  $S(n)$  from the finite-size MPS simulations under the PBCs, for the four selected points  $(J_x/J_z, J_y/J_z) = (0.6, 0.5)$ ,  $(0.8, 0.6)$ ,  $(0.8, 0.7)$  and  $(0.9, 0.8)$  in the  $LL_{xz}$  phase. Here, we have chosen the system size  $L = 50$ , with the bond dimension  $\chi = 30$ .

$S_3$ . Hence, one may restrict to the  $DF_y$  phases. However, we need to tackle two situations separately: on and away from the two characteristic lines:  $J_x/J_z = 0$  with  $J_y/J_z > 0$  and  $J_y/J_z = 1$  with  $J_x/J_z > 0$ .

### 1. The factorized ground states away from the two characteristic lines

From our numerical simulation results, we know that the ground-state wave functions are factorized, which are doubly degenerate in the  $DF_y$  phase, away from the two characteristic lines  $J_x/J_z = 0$  with  $J_y/J_z > 0$  and  $J_y/J_z = 1$  with  $J_x/J_z > 0$ . Given that the Hamiltonian (1) is invariant under the one-site translation operation, a factorized ground state  $|\psi\rangle$  takes the form  $|\psi\rangle = \bigotimes_l |v_1 v_2\rangle_l$  ( $l = 1, \dots, L/2$ ), where  $|v_1\rangle_{2l-1} = s|0_y\rangle_{2l-1} + t|0_z\rangle_{2l-1}$  and  $|v_2\rangle_{2l} = p|0_y\rangle_{2l} + q|0_z\rangle_{2l}$ , respectively, with  $s, p$  being real numbers and  $t, q$  being complex numbers, in order to accommodate the situation that the symmetry under the one-site translation operation is broken. Here, the vectors  $|v_1\rangle_{2l-1}$  and  $|v_2\rangle_{2l}$  have been normalized. That is, we have  $s^2 + t^2 = 1$  and  $p^2 + q^2 = 1$ .

A straightforward calculation yields

$$h_{2l-1,2l}|v_1 v_2\rangle_l = J_x^4 |v_1 v_2\rangle_l + V, \quad (S4)$$

with

$$\begin{aligned} V = & [-J_x J_y s p (J_x^2 + J_y^2 + 3J_z^2) + J_x J_z t q (J_x^2 + 3J_y^2 + J_z^2)] |0_x 0_x\rangle + \\ & [s p (2J_x^2 J_z^2 + J_x^2 J_y^2 + J_y^2 J_z^2 + J_z^4) - J_y J_z t q (3J_x^2 + J_y^2 + J_z^2)] |0_y 0_y\rangle \\ & + [t q (2J_x^2 J_y^2 + J_x^2 J_z^2 + J_y^2 J_z^2 + J_y^4) - J_y J_z s p (3J_x^2 + J_y^2 + J_z^2)] |0_z 0_z\rangle. \end{aligned} \quad (S5)$$

If  $|v_1 v_2\rangle_l$  is an eigenvector of  $h_{2l-1,2l}$ , then  $V$  must vanish. Note that the expectation value of  $h_{2l-1,2l}$  takes the form

$$l \langle v_1 v_2 | h_{2l-1,2l} | v_1 v_2 \rangle_l = J_x^4 + Q, \quad (S6)$$

with

$$Q = (s p J_z - t q J_y)^2 (2J_x^2 + J_y^2 + J_z^2) + J_x^2 (s p J_y - t q J_z)^2. \quad (S7)$$

Accordingly, in order to ensure that  $|v_1 v_2\rangle_l$  is a ground state, we require that  $V = 0$ . If so, we have  $Q = 0$ . Hence, we are led to  $p^2 + s^2 = 1$ . In other words,  $p^2 = t^2$  and  $q^2 = s^2$ . Substituting back into  $V$ , we have  $s p = 0$  and  $t q = 0$ . This implies that either  $s = 0$  and  $q = 0$  or  $t = 0$  and  $p = 0$ . That is, we have

$$\begin{aligned} |v_1\rangle_{2l-1} &= |0_z\rangle_{2l-1}, \\ |v_2\rangle_{2l} &= |0_y\rangle_{2l}, \end{aligned} \quad (S8)$$

or

$$\begin{aligned} |v_1\rangle_{2l-1} &= |0_y\rangle_{2l-1}, \\ |v_2\rangle_{2l} &= |0_z\rangle_{2l}. \end{aligned} \quad (S9)$$

Thus, we have derived the two factorized ground states presented in the main text:  $|\psi_g\rangle = \bigotimes_l |0_y 0_z\rangle_l$  and  $|\psi_g\rangle = \bigotimes_l |0_z 0_y\rangle_l$ , with the ground-state energy per lattice site  $e$  being equal to  $J_x^4$ . Hence, the degenerate ground-state degeneracy is two in the  $DF_y$  phase, consistent with our numerical simulations.

### 2. The factorized ground states on the two characteristic lines

First, we focus on the characteristic line  $J_x/J_z = 0$  with  $J_y/J_z > 0$ . A straightforward calculation yields

$$\begin{aligned} & h_{2l-1,2l} |v_1 v_2\rangle_l \\ &= [s p (J_y^2 J_z^2 + J_z^4) - J_y J_z t q (J_y^2 + J_z^2)] |0_y 0_y\rangle \\ &+ [t q (J_y^2 J_z^2 + J_y^4) - J_y J_z s p (J_y^2 + J_z^2)] |0_z 0_z\rangle. \end{aligned} \quad (S10)$$

Setting  $h_{2l-1,2l} |v_1 v_2\rangle_l = 0$ , we have

$$J_z s p = J_y t q. \quad (S11)$$

Combining with the normalization conditions  $s^2 + t^2 = 1$  and  $p^2 + q^2 = 1$ , we are able to parameterize  $s, t, p$  and  $q$  as follows

$$\begin{aligned} |v_1\rangle_{2l-1} &= \sin \zeta |0_y\rangle_{2l-1} + e^{i\theta} \cos \zeta |0_z\rangle_{2l-1}, \\ |v_2\rangle_{2l} &= \frac{J_y \cos \zeta}{\sqrt{J_y^2 \cos^2 \zeta + J_z^2 \sin^2 \zeta}} |0_y\rangle_{2l} + e^{-i\theta} \frac{J_z \sin \zeta}{\sqrt{J_y^2 \cos^2 \zeta + J_z^2 \sin^2 \zeta}} |0_z\rangle_{2l}, \end{aligned} \quad (S12)$$

where  $\zeta$  and  $\theta$  are two free parameters that are real. We remark that the ground-state energy per lattice site is 0 on the characteristic line  $J_x/J_z = 0$ , with  $J_y/J_z > 0$ .

Next, we turn to the characteristic line  $J_y/J_z = 1$  with  $J_x/J_z > 0$ . The SSB pattern from  $SU(2) \times U(1)$  to  $U(1) \times U(1)$  occurs, with one type-B GM. Here, the staggered  $SU(2)$  symmetry group is generated by the images of  $K_x, K_y$  and  $K_z$  under the cyclic permutation:  $x \rightarrow y, y \rightarrow z$  and  $z \rightarrow x$ . In fact, for a given representation in which one of  $K_x, K_y$  and  $K_z$  is diagonal, we have two factorized ground states that are the highest and lowest weight states, respectively, in this representation. A sequence of degenerate ground states are generated from the action of the lowering operator on the highest

weight state or from the action of the raising operator on the lowest weight state. Actually, such a sequence of degenerate ground states will be explicitly constructed for the staggered SU(2) symmetry group on the characteristic line  $J_x = J_y$  with  $0 < J_x/J_z < J_x^c$  in Sec. E of the SM.

### E. The fractal dimension for highly degenerate ground states on the characteristic line $J_x = J_y$ with $0 < J_x/J_z < J_x^c$

A sequence of degenerate ground states  $|L, M\rangle$  are generated from the repeated action of the lowering operators  $K_-$  on the highest weight state  $|\text{hws}\rangle = (|0_x 0_z \dots 0_x 0_z\rangle + |0_y 0_z \dots 0_y 0_z\rangle)/\sqrt{2}$ :  $|L, M\rangle = 1/Z(L, M)K_-^M|\text{hws}\rangle$ , where  $Z(L, M)$  is introduced to ensure that  $|L, M\rangle$  is normalized. We remark that  $|L, M\rangle$  ( $M = 0, \dots, L/2$ ) span a  $L + 1$ -dimensional irreducible representation of the staggered SU(2) symmetry group.

In order to understand SSB with one type-B GM from an entanglement perspective, the system is partitioned into a block  $\mathcal{B}$  and its environment  $\mathcal{E}$ . Here, the block  $\mathcal{B}$  consists of  $n$  lattice sites that are not necessarily contiguous, with the rest  $L - n$  lattice sites constituting the environment  $\mathcal{E}$ . As a convention, we demand  $n \leq L/2$ . Note that  $|\text{hws}\rangle$ , as an unentangled product state, is split into  $|\text{hws}\rangle_{\mathcal{B}}$  and  $|\text{hws}\rangle_{\mathcal{E}}$ . With this in mind, we introduce the counterparts of the symmetry group SU(2) in the block  $\mathcal{B}$  and the environment  $\mathcal{E}$ , respectively. We define the basis states  $|n, k\rangle$  and  $|L - n, M\rangle$  for the block  $\mathcal{B}$  and the environment  $\mathcal{E}$ , which take the same form as  $Z(L, M)$ . Meanwhile,  $Z(n, k)$  and  $Z(L - n, M)$  need to be introduced to ensure that  $|n, k\rangle$  and  $|L - n, M\rangle$  are normalized.

For the degenerate ground states  $|L, M\rangle$ , we need to introduce a unit cell consisting of two nearest-neighbor sites, due to the staggered nature of the symmetry group SU(2). Therefore, there are two possible configurations:  $|-1_z 0_z\rangle$  and  $|1_z 0_z\rangle$  in the unit cell. Here,  $|\pm 1_z\rangle$  are the eigenvectors of  $S_{z,j}$ , with the eigenvalues being  $\pm 1$ . One may rewrite  $|L, M\rangle$  as follows

$$|L, M\rangle = \frac{M!}{\sqrt{2^M} Z(L, M)} \sum_P (-1)^M \underbrace{|-1_z 0_z \dots -1_z 0_z\rangle}_M \underbrace{|1_z 0_z \dots 1_z 0_z\rangle}_{L/2-M}, \quad (\text{S13})$$

where the sum  $\sum_P$  is taken over all the permutations  $P$  for a given partition  $\{M, L/2 - M\}$ . This allows us to evaluate the norm  $Z(L, M)$ , which takes the form

$$Z(L, M) = \frac{M!}{\sqrt{2^M}} \sqrt{C_{L/2}^M}. \quad (\text{S14})$$

The degenerate ground states  $|L, M\rangle$  admit an exact singular value decomposition:

$$|L, M\rangle = \sum_{k=0}^{\min(M, n/2)} \lambda(L, M, k) |n, k\rangle |L - n, M - k\rangle, \quad (\text{S15})$$

where the singular values  $\lambda(L, M, k)$  take the form,

$$\lambda(L, M, k) = \sqrt{\frac{C_{n/2}^k C_{(L-n)/2}^{M-k}}{C_{L/2}^M}}. \quad (\text{S16})$$

Therefore, the eigenvalues  $\Lambda(L, M, k)$  of the reduced density matrix  $\rho_L(n, M)$  are  $\Lambda(L, M, k) = [\lambda(L, M, k)]^2$ . Hence, the entanglement entropy may be evaluated as follows

$$S_{L(n, M)} = - \sum_k \Lambda(L, M, k) \log_2 \Lambda(L, M, k). \quad (\text{S17})$$

For our purpose, we have to simplify the eigenvalues  $\Lambda(L, M, k)$  by resorting to the normal distribution approximation [S8]

$$C_a^b f^b (1-f)^{a-b} = \frac{1}{\sqrt{2\pi a f(1-f)}} \exp\left[-\frac{(b-af)^2}{2af(1-f)}\right], \quad (\text{S18})$$

where  $af(1-f) \gg 1$ , with  $f = 2M/L$  being a filling factor. Hence, we have

$$\Lambda(L, M, k) = \frac{C_{n/2}^k f^k (1-f)^{n/2-k} C_{(L-n)/2}^{M-k} f^{M-k} (1-f)^{(L-n)/2-(M-k)}}{C_{L/2}^M f^M (1-f)^{L/2-M}} \quad (\text{S19})$$

$$= \frac{1}{n} \frac{1}{\sqrt{\pi\alpha}} \exp\left[-\frac{(k/n - f/2)^2}{\alpha}\right], \quad (\text{S20})$$

where  $\alpha = f(1-f)(L-n)/nL$ . We remark that this approach has been exploited by Popkov and Salerno [S9] to treat the entanglement entropy for the SU(2) spin-1/2 ferromagnetic states. Substituting Eq.(S20) into Eq.(S17) and replacing the sum with an integral, we obtain

$$S_{L(n, M)} = \int_0^1 R \log_2(R/n) dx, \quad (\text{S21})$$

with

$$R = \frac{1}{\sqrt{\pi\alpha}} \exp\left[-\frac{(x-f/2)^2}{\alpha}\right]. \quad (\text{S22})$$

For large  $n$ , Eq.(S21) becomes

$$S_{L(n, M)} = \frac{1}{2} \log_2[\pi e f(1-f)] + \frac{1}{2} \log_2[n(1-n/L)]. \quad (\text{S23})$$

In the thermodynamic limit  $L \rightarrow \infty$ ,  $S_{L(n, M)}$  should be replaced by  $S_f(n)$ , which scales with the block size  $n$  as follows

$$S_f(n) = \frac{1}{2} \log_2[\pi e f(1-f)] + \frac{1}{2} \log_2 n. \quad (\text{S24})$$

This confirms that the fractal dimension  $d_f$  [S10] is identical to the number of type-B GMs  $N_B$ :  $d_f = N_B = 1$  for highly degenerate ground states on the characteristic line  $J_x/J_z = J_y/J_z$  with  $0 < J_x/J_z < J_x^c$ . Here, we remark that  $J_x^c \approx 0.377$ , as follows from the iTEBD simulations.

The same treatment also works for highly degenerate ground states, as a result of SSB from the staggered SU(2) symmetry group to the residual symmetry group U(1) on the characteristic line  $J_y = J_z$  with  $0 < J_x/J_z < 1$ .

*Acknowledgements.* We thank Murray Batchelor, John Fjaerestad and Ian McCulloch for enlightening discussions.

- 
- [S1] Y.-W. Dai, Q.-Q. Shi, H.-Q. Zhou, and I. P. McCulloch, arXiv:2201.01434 (2022).
- [S2] Q.-Q. Shi, Y.-W. Dai, S.-H. Li, and H.-Q. Zhou, arXiv:2204.05692 (2022).
- [S3] G. Fáth and J. Sólyom, Phys. Rev. B **44**, 11836 (1991); B. Sutherland, Phys. Rev. B **12**, 3795 (1975); M. N. Barber and M. T. Batchelor, Phys. Rev. B **40**, 4621 (1989); C. D. Batista, G. Ortiz and J. E. Gubernatis, Phys. Rev. B **65**, 180402(R) (2002); I. J. Affleck, J. Phys. Condens. Matter **2**, 405 (1990); L. Takhtajan, Phys. Lett. A **87**, 479 (1982); H. Babujian, Nucl. Phys. B **215**, 317 (1983); M. T. Batchelor and M. N. Barber, J. Phys. A: Math. Gen. **23**, L15 (1990); B. Aufgebauer and A. Kluemper, J. Stat. Mech. **2010**, P05018 (2010); R. Lundgren, J. Blair, P. Laurell, N. Regnault, G. A. Fiete, M. Greiter, and R. Thomale, Phys. Rev. B **94**, 081112 (2016); R. Thomale, S. Rachel, B. A. Bernevig, and D. P. Arovas, J. Stat. Mech. **2015**, P07017 (2015).
- [S4] G. Vidal, Phys. Rev. Lett. **98**, 070201 (2007).
- [S5] F. Verstraete, D. Porras, and J. I. Cirac, Phys. Rev. Lett. **93**, 227205 (2004).
- [S6] C. H. Bennett, H. J. Bernstein, S. Popescu, and B. Schumacher, Phys. Rev. A **53**, 2046 (1996).
- [S7] P. Calabrese and J. Cardy, J. Stat. Mech. P06002 (2004).
- [S8] A. O. Allen, *Statistics and Queueing Theory* (Academic Press, Inc., New York, 1990), Chap. 3, p. 160.
- [S9] V. Popkov and M. Salerno, Phys. Rev. A **71**, 012301 (2005).
- [S10] O. A. Castro-Alvaredo and B. Doyon, Phys. Rev. Lett. **108**, 120401 (2012).